

Genetic improvement of tomato by targeted control of fruit softening.

ULUISIK, Selman, CHAPMAN, Natalie H, SMITH, Rebecca, POOLE, Mervin, ADAMS, Gary, GILLIS, Richard B, BESONG, Tabot MD, SHELDON, Judith, STIEGELMEYER, Suzy, PEREZ, Laura, SAMSULRIZAL, Nurul, WANG, Duoduo, FISK, Ian D, YANG, Ni, BAXTER, Charles, RICKETT, Daniel, FRAY, Rupert, BLANCO-ULATE, Barbara, POWELL, Ann LT, HARDING, Stephen E, CRAIGON, Jim, ROSE, Jocelyn KC, FICH, Eric A, SUN, Li, DOMOZYCH, David S, FRASER, Paul D, TUCKER, Gregory A, GRIERSON, Don and SEYMOUR, Graham B

Available from Sheffield Hallam University Research Archive (SHURA) at:

<http://shura.shu.ac.uk/31152/>

This document is the author deposited version. You are advised to consult the publisher's version if you wish to cite from it.

Published version

ULUISIK, Selman, CHAPMAN, Natalie H, SMITH, Rebecca, POOLE, Mervin, ADAMS, Gary, GILLIS, Richard B, BESONG, Tabot MD, SHELDON, Judith, STIEGELMEYER, Suzy, PEREZ, Laura, SAMSULRIZAL, Nurul, WANG, Duoduo, FISK, Ian D, YANG, Ni, BAXTER, Charles, RICKETT, Daniel, FRAY, Rupert, BLANCO-ULATE, Barbara, POWELL, Ann LT, HARDING, Stephen E, CRAIGON, Jim, ROSE, Jocelyn KC, FICH, Eric A, SUN, Li, DOMOZYCH, David S, FRASER, Paul D, TUCKER, Gregory A, GRIERSON, Don and SEYMOUR, Graham B (2016). Genetic improvement of tomato by targeted control of fruit softening. *Nature biotechnology*, 34 (9), 950-952.

Copyright and re-use policy

See <http://shura.shu.ac.uk/information.html>

Genetic improvement of tomato by targeted control of fruit softening

Selman Uluisik¹, Natalie H. Chapman¹, Rebecca Smith^{1†}, Mervin Poole², Gary Adams^{1,9}, Richard B Gillis^{1,9}, Tabot M.D. Besong^{1‡}, Judith Sheldon³, Suzy Stieglmeyer^{4††}, Laura Perez⁵, Nurul Samsulrizal¹, Duoduo Wang¹, Ian D. Fisk¹, Ni Yang¹, Charles Baxter³, Daniel Rickett³, Rupert Fray¹, Barbara Blanco-Ulate⁶, Ann L.T. Powell⁶, Stephen E. Harding¹, Jim Craigon¹, Jocelyn K.C. Rose⁷, Eric A. Fich⁷, Li Sun⁸, David S. Domozych⁸, Paul D. Fraser⁵, Gregory A. Tucker¹, Don Grierson¹, and Graham B. Seymour^{1*}

1. School of Biosciences, University of Nottingham, Sutton Bonington Campus, Loughborough, Leics LE12 5RD, UK

2. Heygates Ltd, Bugbrooke Mills, Bugbrooke, Northampton, NN7 3QH, UK

3. Syngenta Seeds, Jealott's Hill International Research Station, Bracknell, Berkshire RG42 6EY, UK

4. Syngenta Crop Protection, Research Triangle Park, North Carolina 27709, USA

5. School of Biological Sciences, Royal Holloway University of London, Egham Hill, Egham TW20 OEX, UK

6. Plant Sciences Department, University of California, Davis, CA 95616, USA

7. Plant Biology Section, School of Integrative Plant Science, 412 Mann Library, Cornell University, 14853, Ithaca, NY, USA

8. Department of Biology and Skidmore Microscopy Imaging Center, Skidmore College, Saratoga Springs, NY 12866, USA

9. School of Health Sciences, The University of Nottingham, B Floor, South Block Link, Queen's Medical Centre, Nottingham NG7 2HA, UK.

*Correspondence to: graham.seymour@nottingham.ac.uk

† Current address. Valley Produce, Springalls Farm, Reading, Berkshire, RG7 1RN, UK

‡ Current address. Physical Sciences and Engineering Division, King Abdullah University of Science and Technology, Thuwal 23955-6900, Saudi Arabia

†† Current address. Q² Solutions, EA Genomics, 5927 South Miami Blvd, Morrisville, NC 27560, USA.

Controlling the rate of softening to extend shelf-life was a key target for researchers engineering genetically modified (GM) tomatoes in the 1990s, but only modest improvements were achieved. Hybrids grown nowadays contain ‘non-ripening mutations’ that slow ripening and improve shelf-life, but adversely affect flavor and color. We report substantial, targeted control of tomato softening, without affecting other aspects of ripening, by silencing a gene encoding a pectate lyase.

Tomato (*Solanum lycopersicum*) is the fourth most important commercial crop in the world in terms of global net production value; estimated at more than \$50bn¹. Tomatoes form an important part of the human diet, as they are a source of minerals, vitamins and phytochemicals. Tomato breeders use the *ripening inhibitor (rin)* mutation^{2,3} to confer the long shelf life that is vital for the supply chain. Hybrids harboring *rin* produce firm fruits that ripen slowly⁴, but they often have poor flavor, fail to develop full color and have reduced nutritional value. Targeted control over ripening-related texture changes would ideally deliver all of the benefits of long shelf-life, improved transportability and disease resistance, without negative consequences for colour, aroma and taste. We report that a tomato *PL* gene is crucial for fruit softening and that silencing this *PL* alters texture without affecting other aspects of ripening. These findings provide insights into the mechanisms of cell wall remodelling in tomato.

Softening in tomato fruit involves disassembly of polysaccharide-rich cell walls, a reduction in cell-to-cell adhesion and changes in cuticle properties that affect water loss^{5,6}. The precise mechanism of softening, and the importance of each factor, has been the subject of decades of research, but has remained elusive. Sequencing the tomato genome revealed more than 50 structural genes encoding known, or putative, cell-wall modifying proteins that are expressed in developing and ripening fruits⁷. Of these, polygalacturonase (PG), pectin methyl esterase, β -galactanase and expansin were highly expressed during the ripening process, and all have been investigated as candidates for promoting changes in texture. However, silencing their expression in transgenic tomato lines has yielded very small or no detectable changes in fruit softening⁸⁻¹⁵. Silencing of a strawberry gene encoding a pectate lyase (PL), using an antisense approach, was shown to reduce fruit softening¹⁶. However, the role of PL in tomato has never been investigated in any detail, probably because early attempts to detect PL enzyme activity were unsuccessful¹⁷. Using RT-qPCR we found five *PL* genes that are expressed in Ailsa Craig tomato fruits, but only one allele (Solyc03g111690) that was expressed at a high level during ripening (**Supplementary Fig. 1**). Transgenic tomato (cv Ailsa Craig) lines containing a 35S::RNAi construct targeting this *PL* were generated. *PL*::RNAi fruits had reduced *PL* expression (**Fig. 1a**), enzyme activity, (**Fig. 1b**) and significantly (Ftest; $P < 0.001$) increased fruit firmness compared with the control azygous wild type line (**Fig. 1c,d**, see also **Supplementary Fig. 2**). These fruits also retained their integrity following storage for 14 days [AU insert time] at 20°C, indicating potential for improved shelf-life (**Fig. 1e**). The increase in fruit firmness in the *PL*::RNAi lines was substantial when compared with effects on texture found when other tomato cell wall remodelling genes, including *PG*, have been down-regulated¹⁰⁻¹⁵ (see **Supplementary Fig. 3**).

Silencing *PL* resulted in changes in fruit firmness with no obvious effects on either yield or weight, ethylene biosynthesis, colour and total soluble solids compared to the controls (Ftest; $P > 0.05$) (**Supplementary Fig. 4**). No significant changes were found in silenced fruits for measurements of metabolites that influence fruit colour, taste or aroma compared with the azygous wild type control [AU state control] (**Supplementary Table 1, Supplementary Fig. 2 and 5**). The expression of fewer than 120 of c.15000 genes were altered in transcriptomes of the *PL*::RNAi fruits in the orange and red ripe stages compared with the azygous control (**Supplementary Tables 2-6, Supplementary Fig. 6**). In addition to reduction in *PL* expression, *PROTODERMAL FACTOR 2-like* (Solyc06g035940) and *CER1* (Solyc03g065250) were upregulated (**Supplementary Tables 3-6**). Both genes encode proteins likely involved in regulating epidermal and cuticle development, which might

influence water loss and fruit shelf-life^{18,19}. However, the cuticle waxes of *PL::RNAi* and control fruits were not significantly different (**Supplementary Fig. 7**).

We examined the cell walls of wild-type and *PL::RNAi* fruits with light and transmission electron microscopy (**Fig. 2**). Using a chitin oligosaccharide probe²⁰, (COS⁴⁸⁸), which recognizes pectins with regions of de-esterified homogalacturonans (HGs), we observed increased labelling density in the tricellular junction zones of *PL::RNAi* fruit pericarp parenchyma cells compared with the wild-type (**Fig. 2a**). Linear low ester HGs are concentrated in these tricellular regions and are also present in the middle lamellae of plant cells^{21,22}. It is thought that tricellular junction zones are reinforced with these polymers because the biomechanical stresses that drive cell separation are concentrated at the cell corners²¹. Our data indicate that tricellular junctions are major sites of PL action. Immunogold localization of de-esterified HG using a monoclonal antibody (JIM5) revealed increased density labelling in the cell walls of the *PL::RNAi* lines compared with the wild-type (**Supplementary Fig. 8**). Notably, JIM5 labelled 'fibrous' material in the tricellular junction zones of the parenchyma cells of the *PL::RNAi* fruits (**Fig. 2b**). The immunoreactivity of the fibrous material suggests that these fibres might represent aggregates of crosslinked HGs²². *PL*-silenced fruits also had reduced amounts of water soluble pectins (WSP) (**Fig. 2c**), suggesting that more of the pectins in the transgenic fruit walls were covalently associated with the wall matrix. Additionally, the WSP fraction from the *PL::RNAi* fruit had a significantly (t-test; $P < 0.05$) higher average molecular weight (~150 kDa) than that from the control (~88 kDa) (**Fig. 2d**). The molecular weights of the extracted WSP pectins from the *PL::RNAi* fruit were similar to those previously reported from unripe tomato fruits¹⁰. To summarize, our findings indicate that PL activity breaks down crosslinked HG polymers in both tricellular junctions and the middle lamella, thereby enabling the pectic polysaccharides in the cell wall to be further degraded by enzymes such as PG¹⁰, resulting in rapid fruit softening.

By texture analysis of a mapping population derived from a tomato wild species introgression line, IL3-4,²³ we show that the *PL* targeted in our experiments resides under a major quantitative trait locus (QTL) for firm fruit texture (**Supplementary Fig 9 and 10**).

Our findings show, to our knowledge for the first time, that specific control over tomato softening can be achieved without detrimental effects on other aspects of ripening, and provide a strategy for breeding tomatoes with an extended shelf-life, while maintaining optimum flavor. The *PL::RNAi* fruits also provide insights into the mechanism of tomato cell-wall remodeling during ripening. Taste tests will be needed to discover whether flavor of *PL*-silenced fruits is affected, but this would best be done using elite lines²⁴. Modulating *PL* expression using natural variation, TILLING (Targeting Induced Local Lesions in Genomes) or genome-editing approach could bring the product to market. Indeed, initial experiments with CRISPR/Cas9-induced mutations in *PL* in transgenic tomato lines confirm the effectiveness of CRISPR edited alleles to alter firmness without affecting other aspects of ripening (**Supplementary Fig. 11**).

ACKNOWLEDGEMENTS

SU was funded by Ministry of Education of the Turkish Republic. The work was part funded by BBSRC and Syngenta Seeds Ltd through a BBSRC 'stand-alone LINK' grants to PDF and GBS (BB/J015598/1 and BB/J016071/1). As part of the BBSRC grant, Syngenta staff (J.S., S.S., C.B. and D.R.) provided support with generating the transgenic plants, the bioinformatics analysis, the microscopy and writing the paper. . GBS and PDF acknowledge support from EU project FP6 EUSOL and the European Cooperation in Science and Technology (COST) Action FA1106. DD was funded by National Science Foundation (USA) grants NSF-MRI 1337280 and NSF-MRI 0922805. BB-U and ALTP were funded by National Science Foundation (USA) grants IOS 0957264 and IOS 0544504. JR was funded by a grant (IOS-1339287) from the Plant Genome Research Program of the National Science Foundation (USA). We acknowledge Syngenta Crop Protection, Research Triangle Park, North Carolina USA, Mariana Franco for cDNA library preparation and Junjian Ni for RNAseq quality checks, read alignment and

gene counting. We acknowledge Jonathan Jones, Vladimir Nekrasov and Sophien Kamoun, TSL and The Gatsby Charitable Foundation for provision of the CRISPR / Cas 9 vectors. We also thank Malcolm Bennett and John Labavitch for useful discussions.

AUTHOR CONTRIBUTIONS

S.U., N.C., R. S., M. P., G. A., R. B.G, T.M.D.B, J.S., S.S., N.S., D.W.,L. P., I.D.F., N.Y., B.B-U.,E.F, L.S, D.D. performed the experiments and data analysis, J.C., statistical analysis. G.B.S. conceived and directed the project and G.B.S, J.C., D.G, C. B., D.R., R. F., A.L.T.P, S.E.H., P.D.F., G.A.T. and J.K.C.R. wrote the MS.

COMPETING FINANCIAL INTERESTS

J.S, S.S, C.B and D.R were full-time employees of Syngenta Seeds Ltd at the time of the study.

FIGURE LEGENDS

Figure 1: Silencing pectate lyase (PL) inhibits tomato fruit softening and could increase shelf-life. **(a)** Levels of *PL* mRNA in control azygous Ailsa Craig (WT) and transgenic *PL::RNAi* fruit at mature green (MG), breaker (BR), breaker + 4 days (BR4) and breaker +7 days (BR7), *PL* transcript levels in the RNAi line are plotted on a difference scale from WT, **(b)** PL enzyme activity from cell wall BR7 extracts in WT and *PL::RNAi* shown as the difference in OD at 232nm, see Methods **(c)** outer and **(d)** inner pericarp maximum load measurements at various stages of ripening in azygous wild type control (WT, orange bars) and *PL::RNAi* (green bars) fruits. For RNA and enzyme measurements, error bars are s.e.m, based on three individual fruit of each genotype (shown as dots). For the texture determinations where there were more fruits (n=26 WT-MG, 12 WT-BR, 8 WT-BR4, 11 WT-BR7 and 24 PL-MG, 25 PL-BR, 26 PL-BR4, 23 PL-BR7) dots represent plant means. Significant ($P < 0.001$; F test) differences in pericarp texture between *PL::RNAi* and WT fruits at a specific developmental stages are indicated by ***. The data were obtained from tomato plants grown in a single trial in spring 2014, transgenic line PL5. **(e)** WT Ailsa Craig and *PL::RNAi* fruits harvested at BR7 were stored at room temperature for 14 days. Scale bar 1 cm.

Figure 2: The mechanism of PL action. **(a)** Detection of demethylesterified homogalacturonan (white arrows) in pericarp cell walls of azygous(WT) and *PL::RNAi* BR7 with a chitosan oligosaccharide COS⁴⁸⁸ pectin probe and calcofluor white for imaging cellulose. Panels show separate labelling and merged images, including enlarged view of tricellular junction area. **(b)** TEM images (left) showing parenchyma cells (PC) from the RNAi line with a tricellular junction (TCJ). A higher magnification view (right) showing fibrous material (black arrows) within tricellular junction labelled with JIM5, a monoclonal antibody against demethylesterified homogalacturonan. **(c)** Levels of water soluble pectin extracted from cell wall preparations and **(d)** their weight average molecular weight from red ripe BR7 control azygous WT (orange) and *PL::RNAi* fruits (green). Error bars are s.e.m, with measurements based on three individual fruits of each genotype (shown as dots). Significant

($P < 0.05$; two-tailed t-test) differences between *PL::RNAi* and WT fruits are shown by *. The data were obtained from tomato plants grown in spring 2013, transgenic line PL5.

-
1. Vincent, H. *et al. Biological Conservation* **167**, 265-275 (2013).
 2. Robinson, R. W., & Tomes, M. L. *Genet. Coop.* **18**, 36-37 (1968).
 3. Vrebalov, J. *et al. Science* **296**, 343-346 (2002).
 4. Kitagawa, M. *et al. Physiologia Plant.* **123**, 331-338 (2005).
 5. Seymour, G.B. Østergaard, L., Chapman, N.H., *et al. Annu. Rev. Plant Biol.* **64**, 219-241(2013).
 6. Martin, L.B.B. & Rose, J.K.C. *J. Expt. Bot.* **65**, 4639-4651 (2014).
 7. The Tomato Genome Consortium. *Nature* **485**, 635-641 (2012).
 8. Smith, C.J.S., *et al. Nature* **334**, 724-726 (1988).
 9. Sheehy, R.E., Kramer, M. & Hiatt, W.R. *Proc. Natl. Acad. Sci.* **85**, 8805-8809 (1988).
 10. Smith, C.J.S. *et al. Plant Mol. Biol.* **14**, 369-379 (1990).
 11. Tieman, D.M., Harriman, R.W., Ramamohan, G. & Handa, A.K. *Plant Cell* **4**, 667-679 (1992).
 12. Tieman, D.M. & Handa, A.K. *Plant Physiol.* **106**, 429-436 (1994).
 13. Hall, L.N. *et al. Plant J.* **3**, 121-129 (1993).
 14. Smith, D.L., Abbott D.A. & Gross K.C. *Plant Physiol.* **129**, 1755-1762 (2002).
 15. Brummell, D.A. *et al. Plant Cell* **11**, 2203-2216 (1999).
 16. Jiménez-Bermúdez, S. *et al. Plant Physiol.* **128**, 751-759 (2002).

17. Besford, R.T. & Hobson, G.E. *Phytochem.* **11**, 2201-2205 (1972).
18. Abe, M., Katsumata, H., Komeda, Y. & Takahashi, T. *Development* **130**, 635-643 (2003).
19. Yeats, T.H. & Rose, J.K.C. *Plant Physiol.* **163**, 5 (2013).
20. Mravec, J. *et al.* *Development* **141**, 4841-4850 (2014).
21. Willats, W.G.T., *et al.* *J. Biol. Chem.* **276**, 19404-19413 (2001).
22. Jarvis, M.C., Briggs, S.P.H. & Knox, J.P. *Plant Cell Environ.* **26**, 977-989 (2003).
23. Eshed, Y. & Zamir, D. *Euphytica* **79**, 175-179 (1994).
24. Causse, M. *et al.* *J. Fd. Sci.* **75**, S531-S541.

ONLINE METHODS

Plant Material

All tomato lines were grown in the UK under standard glasshouse conditions of 16 hours day length, day temperature of 20°C, and night temperature of 18°C with supplemental lighting where required. At least three plants from each genotype were grown in "Pro C" coarse potting compost (Levington) in 7.5 L pots with irrigation supplemented with Vitax 214 with pot locations randomised throughout the glasshouse. Fruit were tagged at the first sign of colour (breaker) and harvested for physical, biochemical and molecular evaluation at various days post breaker, e.g. breaker + 4 (orange ripe) and breaker + 7 (red ripe). *Solanum lycopersicum* cv M82, and the *Solanum pennellii* introgression lines (ILs)²³ were obtained from the Tomato Genetics Resource Centre, Davis, USA (<http://tgrc.ucdavis.edu/>). The M82 x IL3-4 F₂ mapping population was generated in the current study. *Solanum lycopersicum* cv Ailsa Craig was used to generate the pectate lyase (PL) RNAi lines. Plant material was collected and immediately frozen in liquid nitrogen and stored at -80°C for the molecular analyses.

Generation of transgenic pectate lyase (PL) lines

The full length sequence of the PL gene (Solyc03g111690.2) was obtained from www.solgenomics.net. The PL gene specific fragment for RNAi was amplified from breaker fruit cDNA (primers in table S8). Gateway cloning (Invitrogen) was utilized with the plasmid pK7GWIWG2, which has the 35S promoter, as a destination vector. Transgenic tomato plants (cv. Ailsa Craig) were obtained through University of California. (The Ralph M. Parsons Foundation, Plant Transformation Facility). Plantlets were confirmed as harbouring the appropriate transgene by PCR. Single integration events and homozygous lines were selected by quantitative PCR.

Genetic mapping of the fruit texture QTL on IL3-4

A total of 3000 M82 x IL3-4 F₂ seedlings were screened using a combination of Taqman probes and cleaved amplified polymorphic sequences designed to markers TG599, TG42 and CT243 that delineated and occurred within the IL3-4 introgression (<https://solgenomics.net>) to allow for the identification of recombinants. A total of 96 recombinant individuals were identified and these were grown to fruiting and ten fruits per line were tagged at the breaker stage and harvested after 7 days and assessed for weight, colour, texture, and % Brix. The F₃ seeds from the recombinant lines were collected and the progeny screened to identify homozygous quantitative trait loci near isogenic lines (QTL-NILs). At least six fruit from each line were phenotyped for texture and colour to derive the mapping interval containing the texture QTL and a summary of the key recombinants is shown in **Supplementary Fig. 9 and 10**. The sites of recombination in these QTL-NILs were defined by molecular markers using information from the tomato genome assembly (2.40V and 2.50V) on the Sol Genomics Network Website (<http://www.sgn.cornell.edu/>) (**Supplementary Table 8**).

Physiochemical Analysis

Fruit colour was measured using a Minolta Chroma Meter and % Brix by a hand held refractometer. For ethylene analysis, fruits were harvested and stored in sealed containers for 1h. A 1 mL sample of head space was then used for ethylene determination by gas chromatography based on the method of Ward et al,²⁵. For shelf life determinations fruits were harvested from the different lines at Br+7 stage and pooled (6-7 tomatoes) and held at room temperature.

Mechanical measurement of fruit texture

The mechanical properties of fruit were investigated using probe penetration tests on 6mm equatorial sections of the outer and inner pericarp. This followed the method described in Chapman et al ²⁶ where a 1.6 mm flat head cylindrical probe mounted on a 10N load cell is driven into the tissue at a constant speed and for a specific distance and the force required is then measured. The inner pericarp is defined by us as the cells between the vascular boundary and the endodermis and the outer pericarp as those below the skin, but before the vascular boundary.

Determination of PL enzyme activity

For preparation of the acetone insoluble solids (AIS), 20g of fresh pericarp (breaker+7) was homogenised with cold 80% of acetone. The sample was washed with 100% acetone to remove all pigment and the powder left overnight to dry at room temperature. Then 40 mg of the AIS was stirred for 30 min in 1.9 ml of 8.5 M Tris-HCL at 20°C. The samples were then centrifuged for 30 minutes at 14000 rpm, and the absorbance of clear supernatant was measured at 232 nm, for determination of the level of reaction products with double bonds released as a result of PL activity

^{27, 28}

DNA and RNA extraction

DNA was extracted from leaf material using the DNAeasy Plant Mini Kit (Qiagen) according to the manufacturer's instructions. For RNA extraction the RNeasy Plant Mini Kit (Qiagen) was used for samples up to breaker + 4 and the RiboPure™ RNA Purification Kit (Life Technologies) was used for red ripe fruits. RNA was treated with RNase-free DNase (Qiagen) according to the manufacturer's instructions. The concentration of RNA was determined using an Agilent Bioanalyser 2100 (Agilent Technologies). First-strand complementary DNA (cDNA) was synthesized from 0.5 µg of total RNA using 0.5 µg of random hexamers (Promega) in a 15-µL volume and incubated at 70°C for 5 min, followed by the addition of 0.5 mM deoxyribonucleotide triphosphates (Promega), 25 units of RNase inhibitor (Promega), 5 µL of Moloney Murine Leukemia Virus reverse transcriptase (MMLV) buffer X5 (Promega), 1 µL of MMLV reverse transcriptase (Promega), and made up to 25 µL with distilled water. The mixture was incubated at 25°C for 10 min, followed by 42°C for 1 h.

Q-RT-PCR was used to determine expression levels of PL. Three fruits at each stage of ripeness from each line were taken at the different developmental stages. Primers and dual-labelled fluorescent probes (5'FAM and 3'TAMRA) were designed using Primer3 (<http://frodo.wi.mit.edu/>). The PCR reaction contained a 5-µL cDNA pool, 7.5 µL of 2X LightCycler480 Probe Master (Roche Applied Science), 10 mM forward primer, 10 mM reverse primer, and 10 mM probe in a final volume of 15 µL. Elongation factor gene primers were included in each reaction as an internal standard. Standard curves for each gene were run concurrently. TaqMan quantitative RT-PCR was run on a LightCycler480 System (Roche Applied Science), and PCR conditions consisted of an initial denaturation step at 95°C for 10 min, followed by 45 cycles of 95°C for 10 s, 60°C for 50 s, and 72°C for 1 s, and a final cooling step of 40°C for 10 min. Standard curves were used to calculate relative

mRNA concentrations from crossing point values using absolute quantification with LightCycler480 software release 1.5 (Roche Applied Science) and normalized to the reference gene EF (Supplementary Table 8)

RNASeq analysis

RNA was prepared as described above. The resulting cDNA was cleaned using Ampure XP magnetic beads. It was fragmented to about 400bp using a Covaris S2 instrument and ligated to adapters using an Apollo 324 instrument and PrepX ILM DNA Library Kit. PCR amplification was performed using KAPA HiFi HotStart ReadyMix (2X). Six samples were pooled per lane and sequenced using an Illumina HiSeq to generate 100-nucleotide single end sequence reads.

After quality assessment by FastQC ²⁹, untrimmed reads were aligned to the ITAG 2.3 tomato reference genome using Tophat version 2.0.12 ³⁰ with Bowtie2 version 2.2.3 ³¹ i.e., tophat -N 6 -g 6 -no-novel-juncs. On average, 92% of the reads aligned per sample.

Reads aligned to annotated regions were counted using an in-house gene counting algorithm. Gene counts were then normalized using the R Bioconductor package EDASeq version 2.0.0 normalizing between lanes ³².

Differentially expressed genes were determined by the R Bioconductor package edgeR version 3.8.4 ³³. To control the family-wise error rate, p-values were adjusted for multiple comparisons using the Benjamini-Hochberg method producing an adjusted p-value or false discovery rate (FDR). An FDR <

0.05 was considered statistically significant. Genes were considered to be differentially expressed if they had an FDR < 0.05 and a log₂ fold change greater than 1 or less than -1 (fold change of 2).

The gene ontology (GO) term enrichment process utilized GO terms extracted from the Gramene BioMart, <http://ensembl.gramene.org/biomart/martview>, as of November 7, 2014. The R Bioconductor package goseq version 1.18.0³⁴ was used to perform GO enrichment analysis on differentially expressed genes from the downloaded terms correcting for gene length bias. RNASeq Fastq files deposited in European Nucleotide Archive accession number PRJEB13836 (<http://www.ebi.ac.uk/ena/data/view/PRJEB13836>).

Metabolite analysis

Extraction and analysis of carotenoids

Carotenoids and tocopherols were extracted from freeze dried fruit. Extractions were made from sample powder (10 mg) in 1.5 mL centrifuge tubes. Metabolites were extracted by the addition of chloroform and methanol (2:1). Samples were stored for 20 min on ice. Subsequently, water (1 vol.) was added. Samples were centrifuged for 5 min at top speed in a Heraeus Pico21 centrifuge (Thermo Scientific). The organic phase, containing the pigment extract, was placed in a fresh centrifuge tube and the aqueous phase re-extracted with chloroform (x2 by volume). Organic phases were pooled and dried using the Genevac EZ. Dried samples were stored at -20°C and dissolved in ethyl acetate prior to chromatographic analysis.

Carotenoids were separated and identified by Ultra High Performance Liquid Chromatography with photo diode array detection (UPLC-PDA). An Acquity™ UPLC (Waters) was used with a BEH C18 column (2.1 x 100 mm, 1.7 μm) with a BEH C18 VanGuard pre-column (2.1 x 50 mm, 1.7μm). The mobile phase used was A: MeOH/H₂O (50/50) and B: ACN (acetonitrile)/ethyl acetate (75:25). All solvents used were HPLC grade and filtered prior to use through a 0.2μm filter. The gradient was

30% A: 70% B for 0.5 min and then stepped to 0.1% A:99.9% B for 5.5 min and then to 30% A:70% B for the last 2 min. Column temperature was maintained at 30°C and the temperature samples at 8°C. On-line scanning across the UV/Vis range was performed in a continuous manner from 250 to 600 nm, using an extended wavelength PDA (Waters). Carotenoids were quantified from dose-response curves. The HPLC separation, detection and quantification of carotenoids, tocopherols and chlorophylls have been described in detail previously³⁵.

Extraction and analysis of intermediary metabolites

Frozen material was freeze-dried and ground to a fine powder by using a tissue lyser (Qiagen). Then, 10 mg of powder was extracted with 1 mL of 50% methanol for 20 min at room temperature and shaking. 1 ml of chloroform was then added and centrifuged at top speed for 3 min to allow phase separation. 20 µL of the polar phase containing intermediary metabolites was transferred to a HPLC glass vial and spiked with 10 µL of the internal standard solution (1 mg/ml of ribitol in methanol). Samples were taken to dryness using a vacuum centrifuge Genevac EZ.27 and stored at -20°C until derivatisation and analysis.

Dried samples were derivatised to their methoxymated and silylated forms³⁶. First, 30 µL of methoxyamine hydrochloride (20 mg/mL in pyridine anhydrous) was added to samples and incubated at 40° C for 1 hr. Following this reaction, samples were treated with 70 µL of MSTFA and heated at 40° C for 2 hr. 1 µl of the final solution was injected into a 7890B gas chromatograph on-line with a 5977A mass spectrometer (Agilent Technologies, Palo Alto, California, US). Metabolites were separated in a DB-5MS 30 m x 250 µm x 0.25 µm column (J&W Scientific, Folsom, California, US) equipped with a 10 m guard column and using a temperature gradient ranging from 70° to 320° C at 5° C/min. Helium was employed as the carrier gas and the flow rate was set at 1 ml/min. The

inlet was heated to 280° C and the mass spectrometer transfer line to 250° C. A mixture of n-alkanes ranging from 8 to 32 carbons was used for retention index external calibration.. Levels of metabolites analyzed by GC/MS were quantified relative to the internal standard and corrected by dried weight of biomass. AMDIS version 2.71 of the software was used for peak deconvolution and identification of metabolites ³⁷.

Determination of cuticular wax levels

Analysis of the cuticular waxes of the ripe fruits of control and PL RNAi lines was carried out as described in ³⁸ . Sections of peel were collected from red ripe breaker + 7 stage azygous wild type control and PL RNAi transgenic tomato fruit, scraped to remove as much cellular material as possible, then air-dried. Wax was extracted from the peels by placing the peels in a beaker with ~100 mL of chloroform containing 100 µg of tetracosane as an internal standard, and swirling for 2 minutes. The peels were then taped flat and scanned to determine their surface area. The wax extract was concentrated by air drying and filtered through chloroform-rinsed filter paper (VWR) . An aliquot of each wax sample was dried by heating at 40°C under a stream of N₂, then derivatized with equal parts pyridine (EMD Millipore) and BSTFA (N,O-bis(trimethylsilyl)trifluoroacetamide) (Sigma) for 30 minutes at 70°C, dried again by heating under N₂, and resuspended in 100 µL of chloroform. The samples were analyzed by gas chromatography using an Agilent GC 6850 with a Flame Ionization Detector. Compound identification was made based on comparisons of retention times with standards and also by performing GC-MS analysis of two of the samples using an Agilent GC 6890 coupled to a JOEL GC MATE II mass spectrometer. Levels of each wax compound were normalized to the internal standard and the surface area of the peels.

Measurement of volatile compounds

Determination of volatile compounds followed the method developed from Buttery et.al.³⁹. Samples were kept at -80 °C and each sample was defrosted and allowed 30 minutes to equilibrate before GC-MS analysis. Volatiles were collected using SPME Fibres (50/30µm DVB/CAR/PDMS, Supelco, Sigma Aldrich, UK) and separated and analysed by GCMS using a ZB-WAX Capillary GC Column (30 m, 0.25mm I.D., 1.00µm Film Thickness) on a Trace 1300 series GC coupled with the Single-Quadrupole Mass Spectrometer (Thermo Fisher Scientific, Hemel Hempstead, UK). Volatiles were identified by comparison of each mass spectrum with spectra in reference collections (Microsoft Windows™ Version 2.0 of the NIST Mass Spectral Search Program for the NIST/EPA/NIH Mass Spectral Library).

Cell Wall Analysis

For the preparation of a crude cell wall material (CWM), fresh tomato pericarp (40g) was peeled, cubed and boiled in 95% EtOH (100 mL) at 80° C for 30 min. The sample was cooled to room temperature, homogenised using a coffee grinder then filtered through Miracloth and washed successively with hot 85% EtOH (200 mL), chloroform:methanol (1:1 v/v) (200 mL) and 100% acetone. The samples were then air dried overnight. For fractionation of tomato CWM, 7.5 mg was placed into tube with 1.5 mL of dH₂O. The sample was stirred 4 hours at room temperature and then centrifuged for 20 minutes at 10,000g. The supernatant which contained the water soluble pectin was filtered through GF/A paper. The supernatant was made to a known volume (1.5 mL) using dH₂O. Uronic acid assays were performed using the method of Blumenkrantz and Asboe-Hansen⁴⁰.

Determination of pectin heterogeneity and molecular weights

Polyuronide heterogeneity and molecular weights were determined as follows. The distribution of the sedimentation coefficients (heterogeneity) were determined from sedimentation velocity analytical ultracentrifugation (rotor speed of 45000 rpm, at 20.0°C in a Beckman (Palo Alto) Optima XL-I win interference optics) and a loading concentration of 0.3mg/mL to minimize any non-ideality effects. The data was analysed using the SEDFIT procedure of Dam & Schuck,⁴¹ and showed all pectin samples to be very polydisperse with material extending to at least 8S and as high as 17S in some cases. To obtain the (weight average) molecular weights sedimentation equilibrium experiments (on the same equipment) were then undertaken on samples from three separate fruits from each treatment at a rotor speed of 15000 rpm, other conditions the same, and data analysed using the SEDFIT-MSTAR procedure of Schuck, Harding and co-workers⁴² to estimate the weight average molar masses for pectic polysaccharides.

Immunocytochemistry

Tomato fruit were harvested at Breaker +7 and 2 mm cubes of pericarp tissue were fixed in 0.1M Sodium Cacodylate Buffer, 2% Paraformaldehyde, pH6.9 overnight at 4°C. The tissue samples were then dehydrated through an Ethanol series and embedded in LR White resin prior to sectioning.

Light microscopy/COS⁴⁸⁸ labelling - 0.5 µm sections were cut using a diamond knife (Diatome, USA) on a Leica ultramicrotome and collected onto the wells of 10-welled immunoslides (Electron Microscopy Sciences, Ft. Washington, PA, USA) coated with poly-L-lysine (Sigma Chemical; St. Louis,

MO, USA). After drying at room temperature for 2h, the sections were incubated for 30 min in 50 mM MES buffer (pH 5.7), labelled with COS⁴⁸⁸ diluted 1/1000 in MES buffer for 90 min in the dark at room temperature (COS was kindly provided by Jozef Mravec and William G. T. Willats of the Department of Plant and Environmental Sciences of the University of Copenhagen) and subsequently washed three times with MES buffer. The sections were subsequently labelled for 2 min in 1 µg/mL Calcofluor dissolved in deionized water and washed three times with deionized water. The sections were covered with a coverslip and viewed with an Olympus Fluoview 1200 confocal laser scanning microscope. Merged images of COS⁴⁸⁸ and Calcofluor labelling were obtained using the Olympus Fluoview 1200 software program.

Transmission Electron Microscopy (TEM) - 60 nm sections were cut using a diamond knife with a Leica Ultramicrotome and collected on Formvar coated nickel grids. The sections were then immunolabelled using JIM5 (Plant Probes, Leeds, UK) as described in ⁴³. The sections were stained for 2 min in uranyl acetate, washed extensively with deionized water and dried before viewing on a Zeiss Libra 120 TEM. For control experiments, the primary antibody was eliminated from the labelling protocol.

Statistical Analysis

The mechanical measurements of fruit texture and other storage properties were analysed as the dependant variables in linear mixed models, fitted using the Restricted Maximum Likelihood (REML) routines in the Genstat 17 statistical package. The independent variables fitted as fixed effects were genotype and ripening stage and the individual plants and fruits within plants were included as random effects in the model. The covariance model takes into account that measurements on fruits

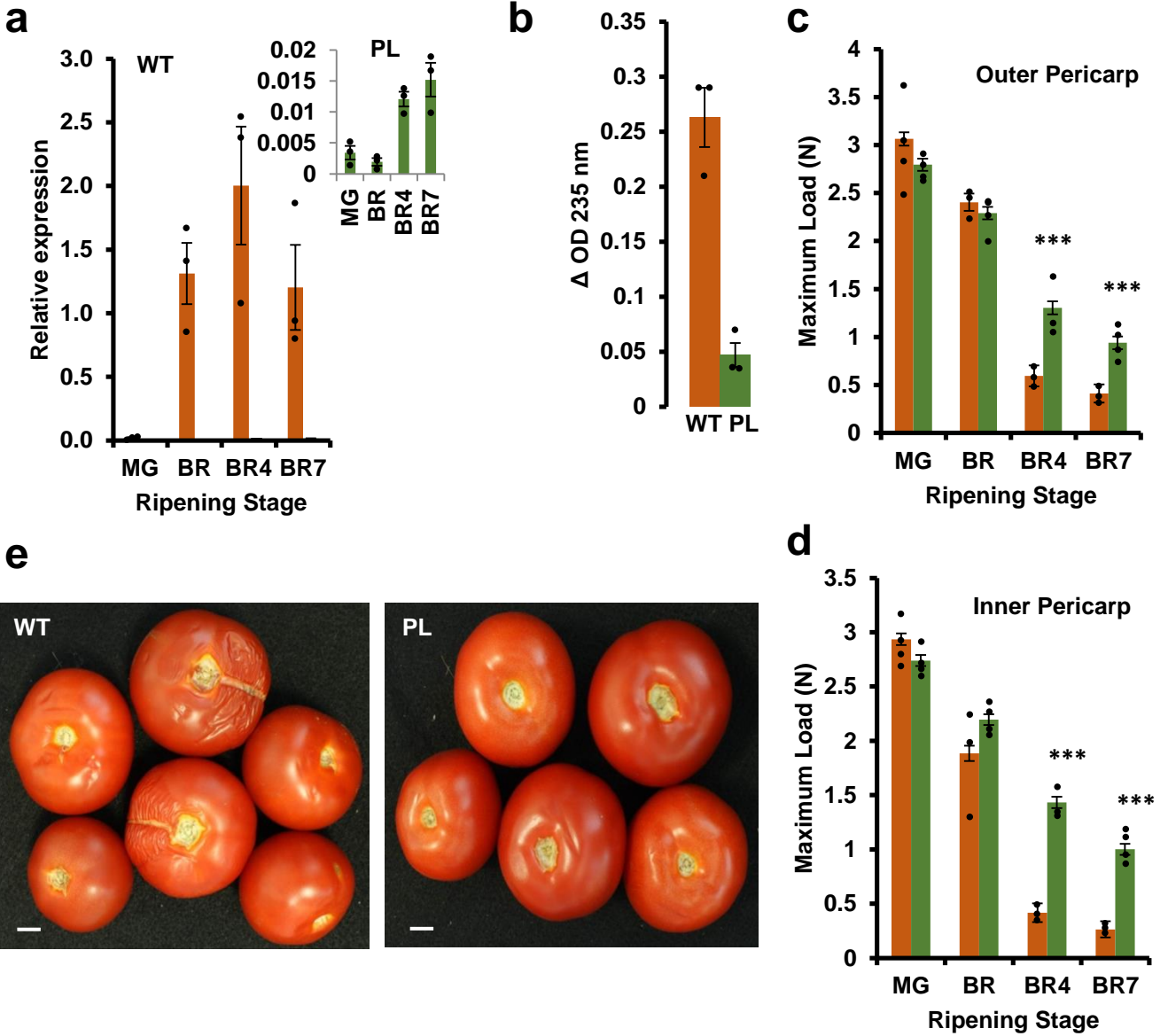
from the same plant were likely to be more highly correlated than those from different plants. It also ensured that the variation between plants of different genotypes was tested against the variation among plants of the same genotype and that the variation among fruits at different stages of ripening and its interaction with genotype was tested against the random variation among fruits of the same genotype. Where pre-planned comparisons between particular groups of genotypes were of interest this was achieved by including orthogonal contrasts describing these comparisons in the fixed effects to further partition the between genotype variation.

References

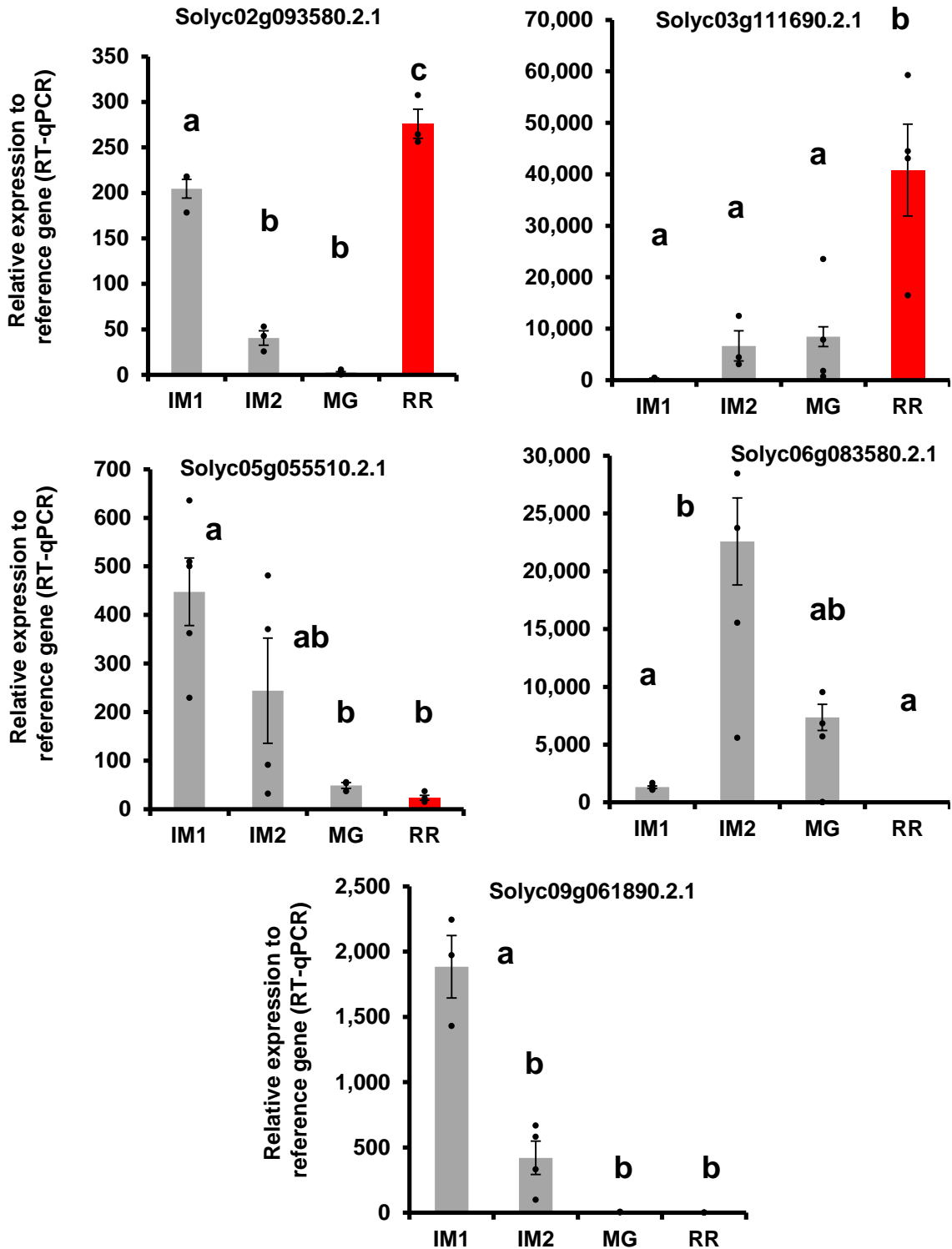
25. Ward, T.M. *et al.* Isolation of Plant Growth Substances 4: Cambridge, UK: Cambridge University Press. pp. 135–151. (1978).
26. Chapman, N.H. *et al.* *Plant Physiol*, **159**, 1644-1657 (2012).
27. Marín-Rodríguez, M.C. *et al.* *Plant Mol Biol*. **51**, 851-857 (2003).
28. Collmer, A., Ried, J.L. & Mount, M.S. *Meth. Enzymol.* **16**, 329-335 (1988).
29. Andrews, S. FastQC: <http://www.bioinformatics.babraham.ac.uk/projects/fastqc> (2010).
30. Trapnell, C., Pachter, L. & Salzberg, S.L. TopHat: *Bioinformatics* **25**, 1105-1111 (2009).
31. Langmead, B. & Salzberg, S. *Nature Methods* **9**, 357-359 (2012).
32. Risso, D., Schwartz, K., Sherlock, G. & Dudoit S. *BMC Bioinformatics* **12**, 480 (2011).
33. Robinson, M.D., McCarthy, D.J. & Smyth, G.K. *Bioinformatics* **26**, 139-140 (2010).
34. Young, M.D., Wakefield, M.J., Smyth, G.K. & Oshlack, *Genome Biol* **11**, R14 (2010).

35. Halket, J.M., Waterman, D., Przyborowska, A.M., Patel, R.K., Fraser, P.D. & Bramley, P.M. *J Exp Bot.* **56**, 219-243 (2005).
36. Fraser, P.D., Elisabete, M., Pinto, S., Holloway, D.E. & Bramley, P.M. *Plant J.* **24**, 551-558 (2000).
37. Perez-Fons, L. *et al. Scientific Reports* **4**, Article number: 3859 (2014).
38. Bolger, A. *et al. Nature Genetics* **46**, 1034-1038. (2014).
39. Buttery, R.G., Teranishi, R. & Ling, L.C. *J. Agric. Food Chem.* **35**, 540-544 (1987).
40. Blumenkrantz, N. & Asboe-Hansen, G. *Anal. Biochem.* **54**, 484-489 (1973).
41. Dam, J. & Schuck, P. *Meth. Enzymol.* **384**, 185-212 (2004).
42. Schuck, P. *et al. SEDFIT–MSTAR: Analyst* **139**, 79-92 (2014).
43. Domozych, D.S., Serfis, A., Kiemle, S.N. & Gretz, M.R. *Protoplasma* **230**, 99-115 (2007).
44. Livak, K.J. & Schmittgen, T.D. *Methods* **25**: 402-8 (2001).
45. Nekrasov V., Staskawicz B., Weigel D., Jones J.D. & Kamoun S. *Nat Biotechnol* **31**: 691-693 (2013).

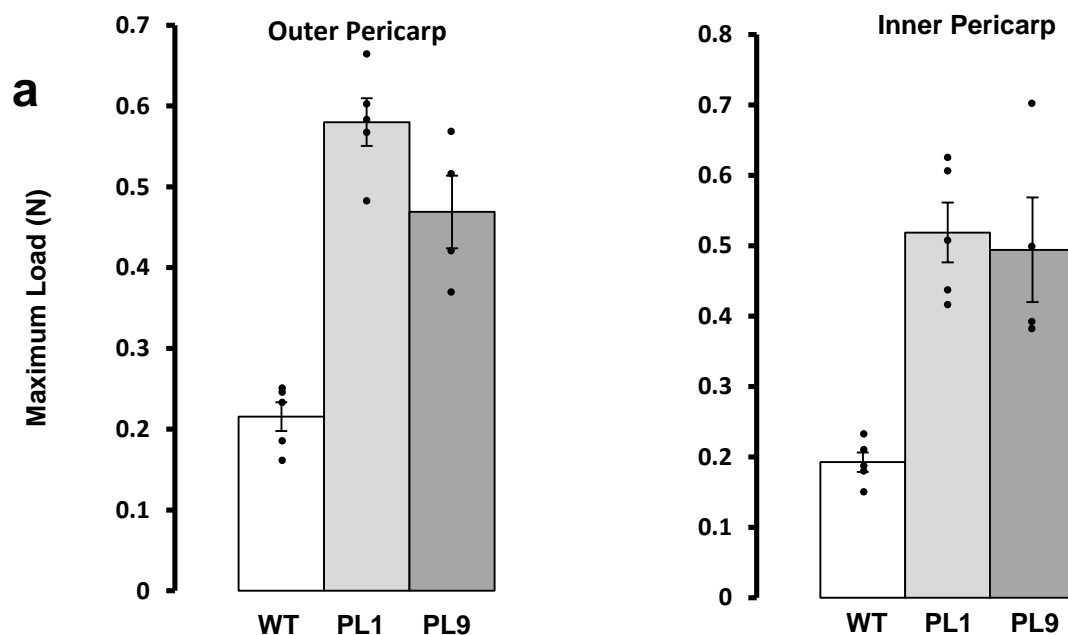
Uluşik et al Fig. 1



Supplementary Figure 1. PL gene expression in tomato fruit.



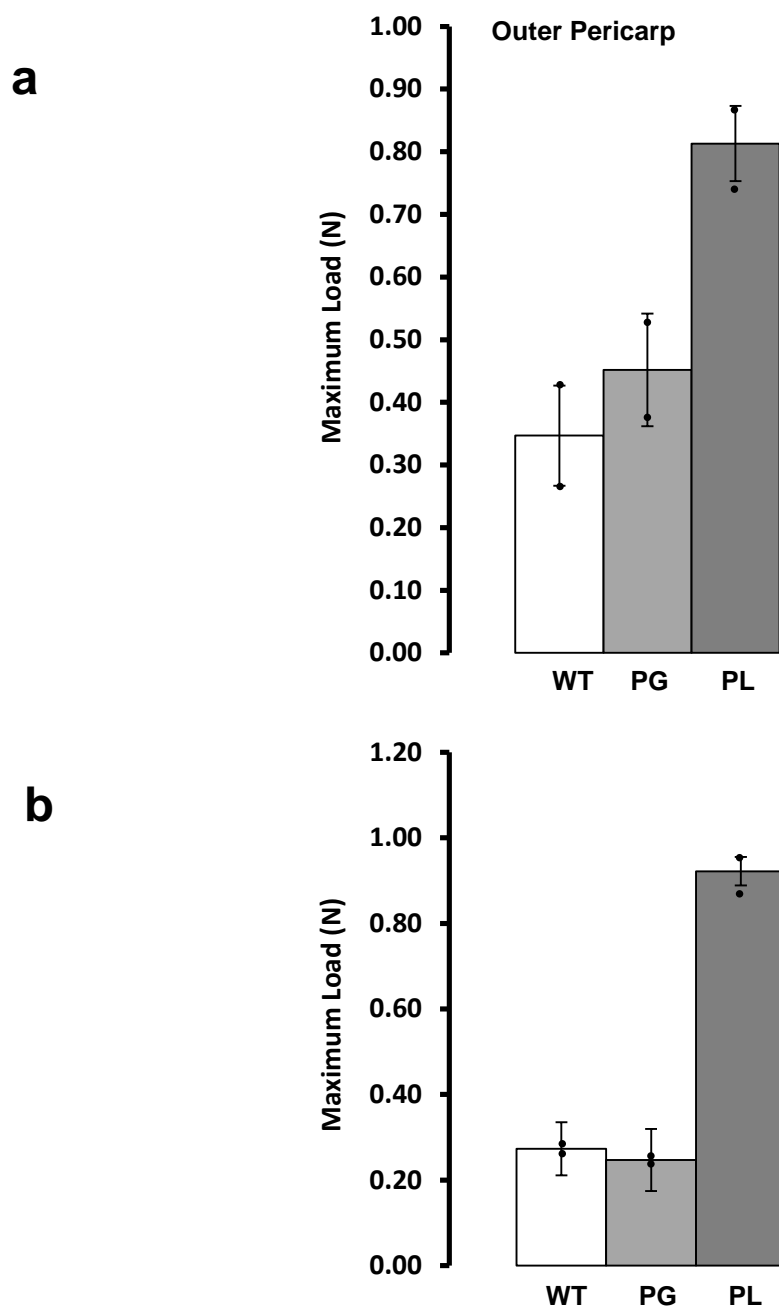
Relative expression of five PL-coding genes measured in at least three fruit of each genotype (cv. Alisa Craig) at four stages of development, immature-1 (IM-1, 10 days post anthesis, dpa), immature-2 (IM-2, 20 dpa), mature green (MG, 31 dpa) and red ripe (RR, breaker +7 days). Individual fruit means shown as dots. Letters correspond to significant differences between stages ($P < 0.05$, two-tailed t-test). Primers for the PL-coding and reference genes are provided in **Supplementary Table 8**. The method of Livak & Schmittgen⁴⁴ was used to account for differences in primer efficiency.

Supplementary Figure 2. Mechanical measures of pericarp texture of two additional independent PL::RNAi transgenic fruit lines.**b**

Key taste and colour metabolites	WT		PL9		PL1	
	Mean	s.e.m	Mean	s.e.m	Mean	s.e.m
$\mu\text{g}/\text{mg}$ DW except lycopene						
Glucose	15.47	1.36	13.67	1.05	13.13	1.18
Fructose	2.72	0.13	2.46	0.10	2.40	0.11
Malic acid	0.07	0.01	0.06	0.01	0.09	0.01
Citric acid	0.26	0.02	0.23	0.02	0.27	0.02
Lycopene ($\mu\text{g}/\text{g}$ DW)	1290.00	109.41	1508.00	84.75	1784*	94.75

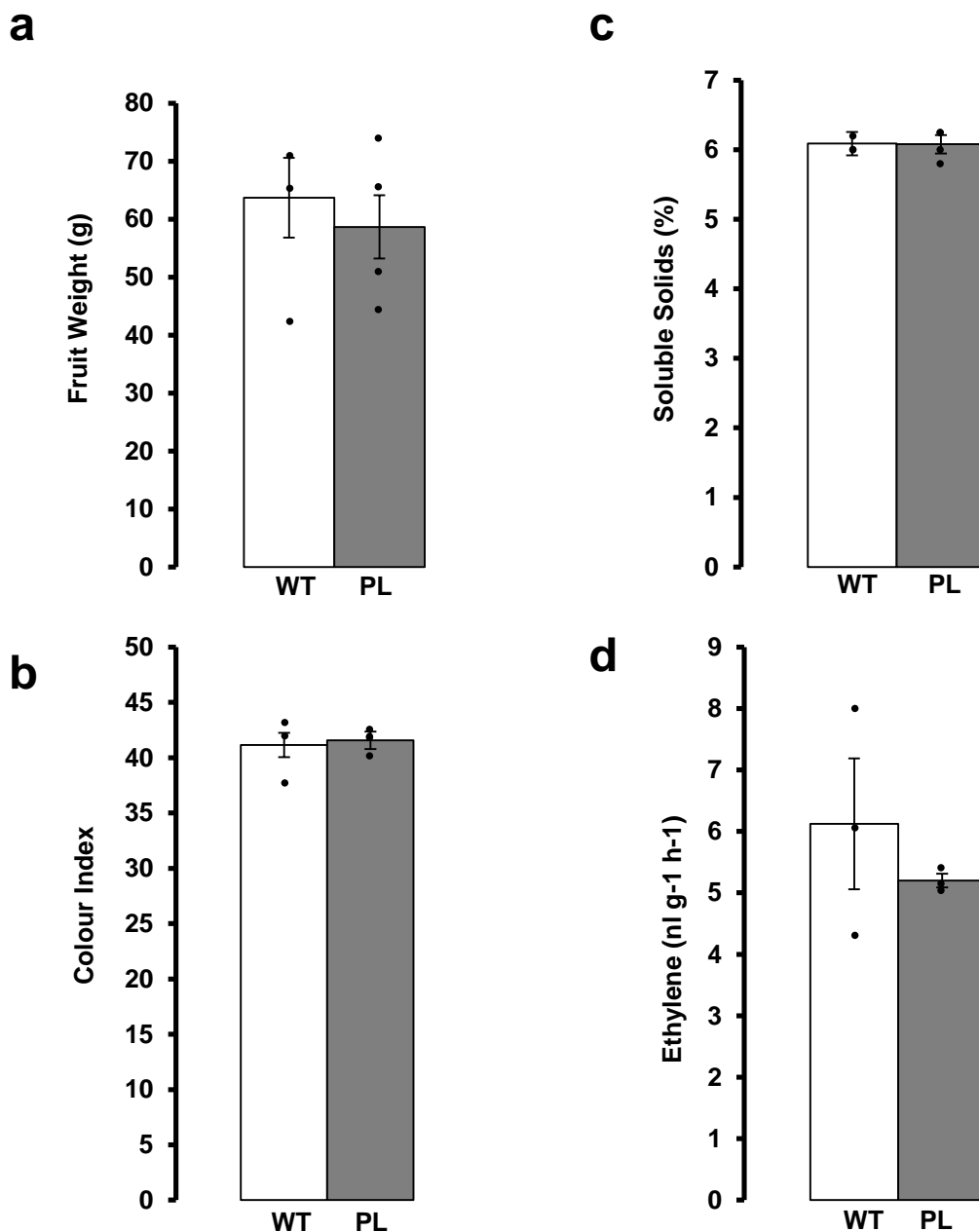
a, Outer and inner pericarp texture based on measuring maximum load in red ripe fruit at breaker + 7 of two additional (to PL5 described in main text) homozygous independent PL transgenic lines (PL1 and PL9) in comparison with an azygous wild type (WT) control. Error bars are s.e.m. based on at least four fruits measured from each genotype represented by dots. **b**, key taste and colour metabolites in breaker + 7 fruits of the two homozygous independent PL transgenic lines (PL1 and PL9) in comparison with an azygous wild type control (WT). There were no significant (Ftest; $P > 0.05$) differences between the transgenic and WT lines, except for lycopene levels in PL 1 alone where a small, but significant (Ftest; $P = 0.02$), increase was apparent in comparison with the control. s.e.m based on four individual fruits for PL1 and five individual fruits for PL9 and three from the WT line. All plants used for the texture and metabolite analyses above were grown summer 2013.

Supplementary Figure 3. Comparison of mechanical measurement of pericarp fruit firmness in PL and PG transgenic lines.



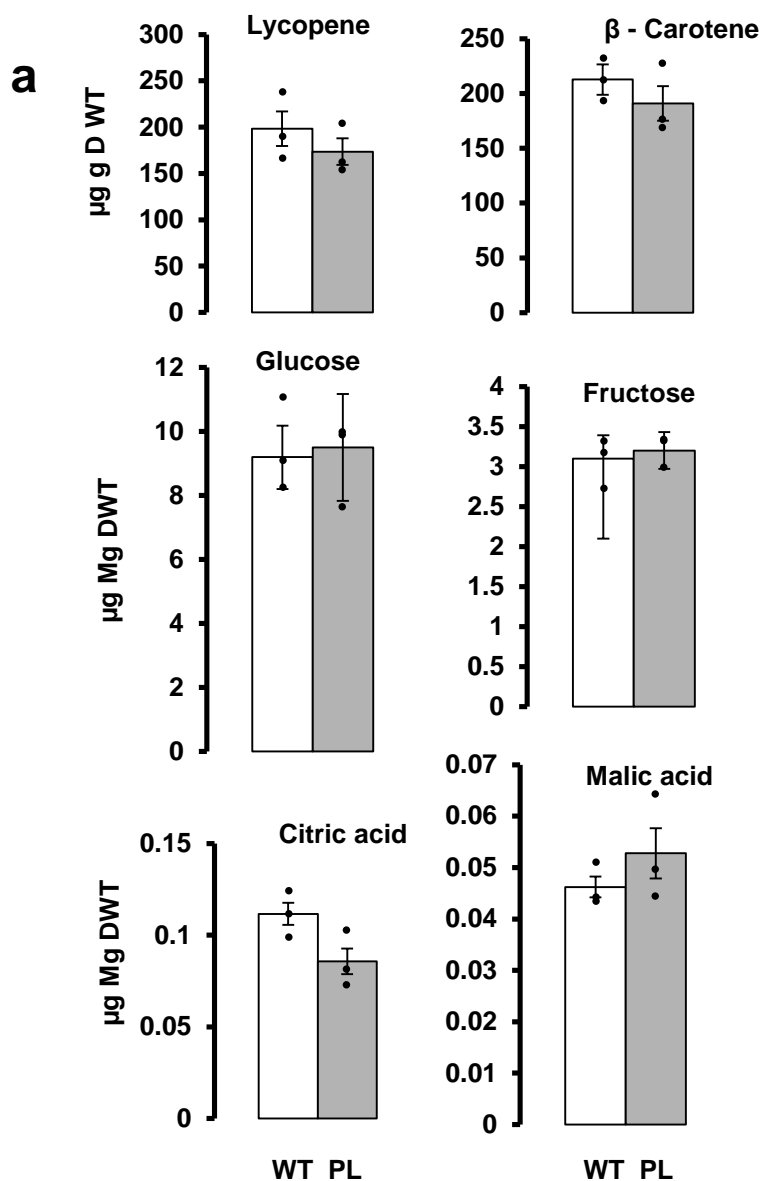
a, Outer and **b**, inner pericarp maximum load of red ripe fruits (breaker + 7 days) from azygous wild type control (WT), the PL::RNAi line PL5 and an antisense polygalacturonase (PG) line where PG expression was suppressed to below 1% of normal levels. Error bars are s.e.m. There were eight fruits of each genotype. Dots represent plant means. There was no significant difference in pericarp firmness between the control and antisense PG lines. The PL::RNAi line was significantly (Ftest; $P < 0.05$) firmer than both PG and control lines.

Supplementary Figure 4: Physiochemical characteristics of WT and PL::RNAi fruits are indistinguishable.



Physiochemical characteristics, **a**, weight, **b**, pericarp skin colour, **c**, total soluble solids of azygous wild type control (WT) and PL::RNAi (PL) red ripe fruits at breaker +7 days and, **d**, fruit ethylene production from orange ripe fruits at breaker + 4 days. Error bars are s.e.m. There were no significant (Ftest; $P > 0.05$) differences between WT and PL fruits. There were four fruits measured from genotype PL5 represented by dots.

Supplementary Figure 5: Metabolite profiles of azygous and PL::RNAi fruits are indistinguishable.

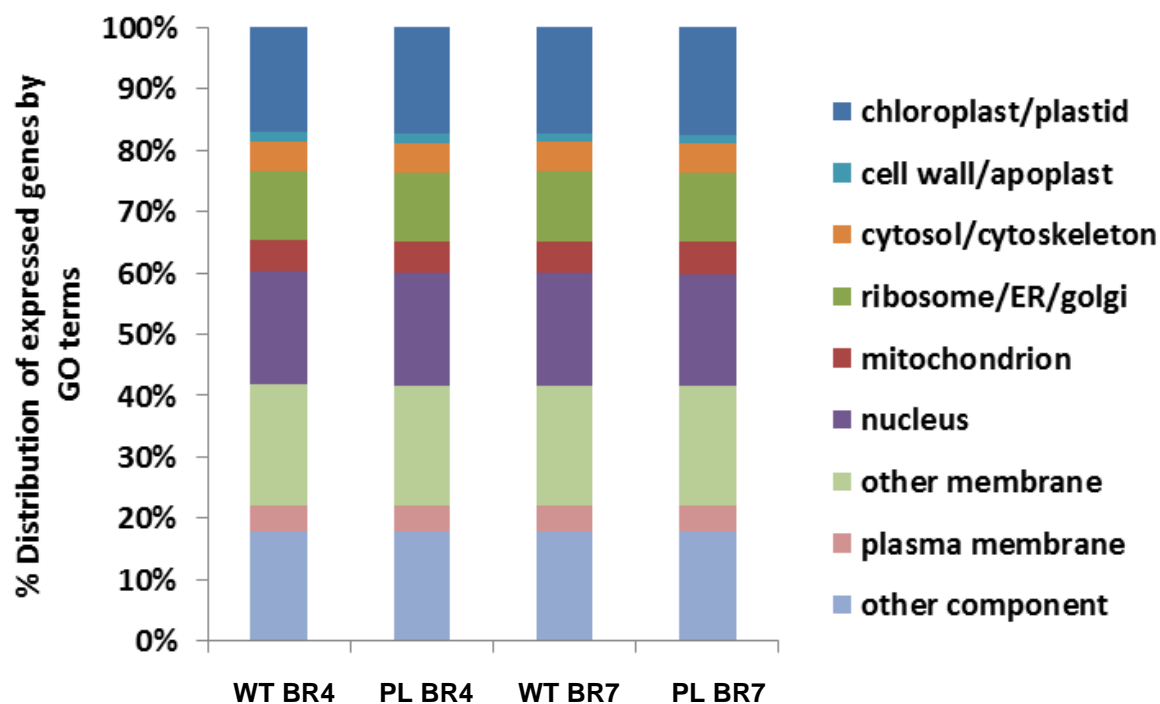


b

Volatile (ppm)	WT PL	
	WT	PL
Hexanal	1.30 ± 0.22	1.42 ± 0.17
trans-2-hexenal	0.45 ± 0.06	0.46 ± 0.12
6-methyl-5-heptene-2-one	0.62 ± 0.10	0.68 ± 0.20
Hexanol	0.07 ± 0.02	0.10 ± 0.02
cis-3-hexen-1-ol	0.15 ± 0.04	0.17 ± 0.04

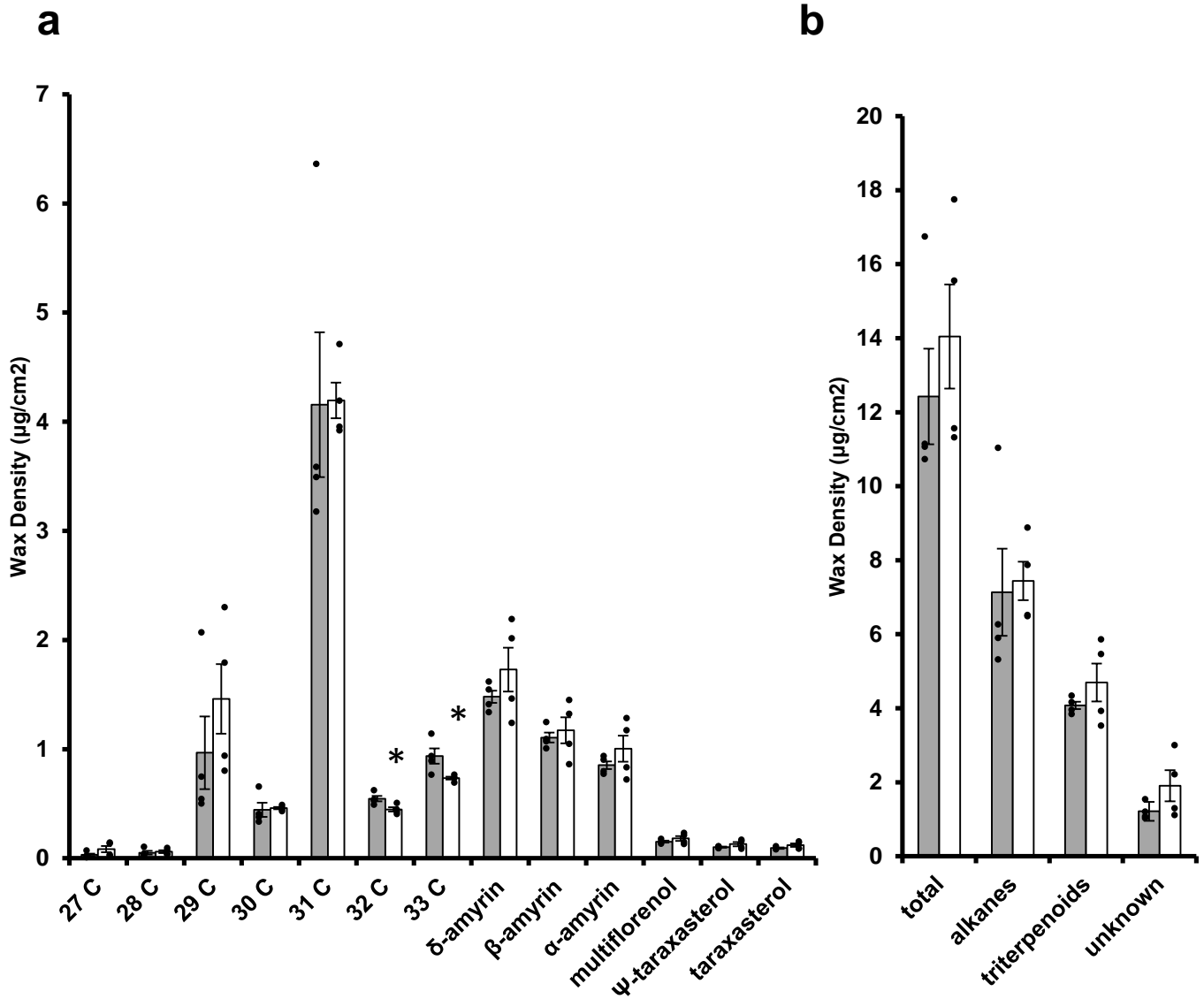
a, Carotenoids, sugars, acid levels and, **b**, volatiles in azygous wild type control (WT) and PL::RNAi (PL) in red ripe fruit at breaker + 7 days (PL). Error bars are s.e.m. There were no significant (Ftest; $P > 0.05$) differences between azygous and PL::RNAi fruits. Three fruits were measured from control and PL5 fruits represented by dots.

Supplementary Figure 6: Summary chart showing transcriptome profiles for azygous and PL::RNAi lines.



Distribution of expressed genes by GO terms from azygous wild type control (WT) and PL::RNAi line PL5 orange ripe fruits (breaker + 4 days) and red ripe fruits (breaker + 7 days) illustrating that the transcriptome profile of the fruit in the two treatments was essentially identical. Three individual fruits were sampled at each stage of ripening for each genotype and analysis of the RNASeq data is presented in detail in Supplementary **Tables 2-7** and in the Methods section.

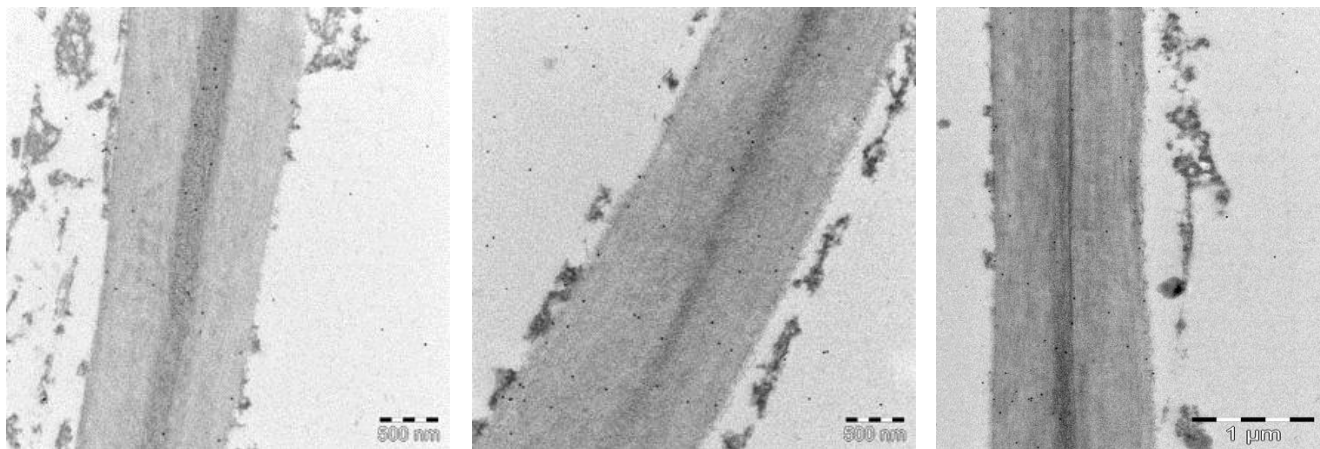
Supplementary Figure 7: The cuticle wax profiles of azygous (red bars) and PL::RNAi (blue bars) red ripe fruits at breaker + 7 days.



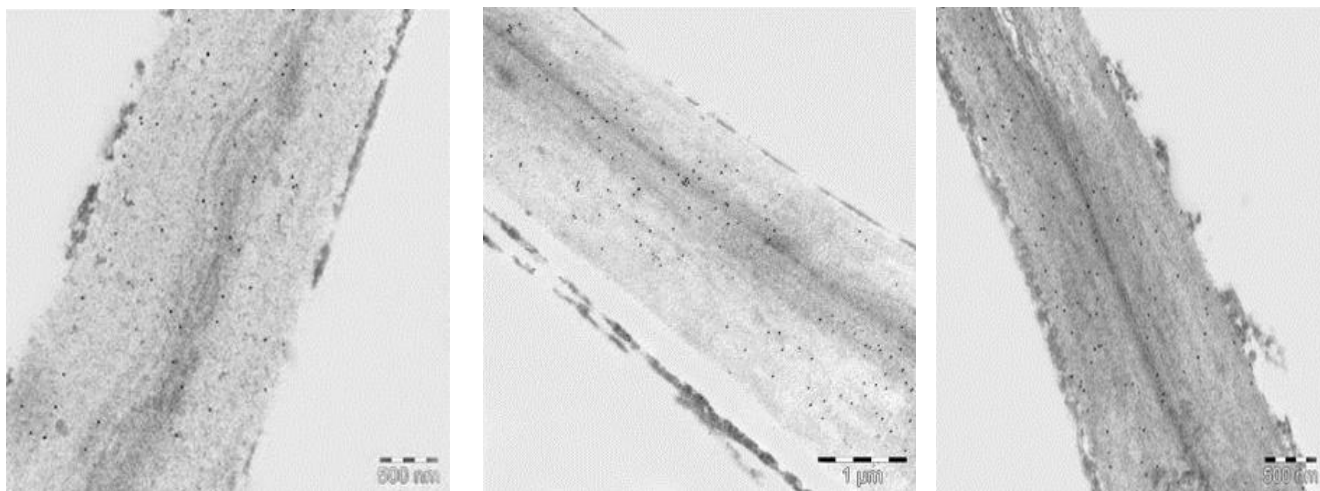
The total amount of wax, **a**, and the levels of alkanes and triterpenoids, **b**, were not significantly different between the azygous wild type control (shaded) and PL::RNAi (clear) bars, as was the case for almost all individual wax compounds. The only statistically significant ($P=0.05$; two-tailed t-test) differences were in the abundance of 32 and 33 carbon alkanes, but the magnitude of the differences were too small to account for the differences in fruit firmness based on transpirational water loss. We conclude that the elevated expression of CER1, which is involved in cuticular alkane biosynthesis in the RNAi line did not have a major effect on cuticle function or composition. Error bars are s.e.m. Four individual fruits, represented by dots, were sampled from the azygous and PL::RNAi PL5 genotypes.

Supplementary Figure 8: Immunogold labelling with JIM5 recognising demethylated homogalacturonan in cell walls of azygous and PL::RNAi pericarp parenchyma cells.

a WT parenchyma cell walls

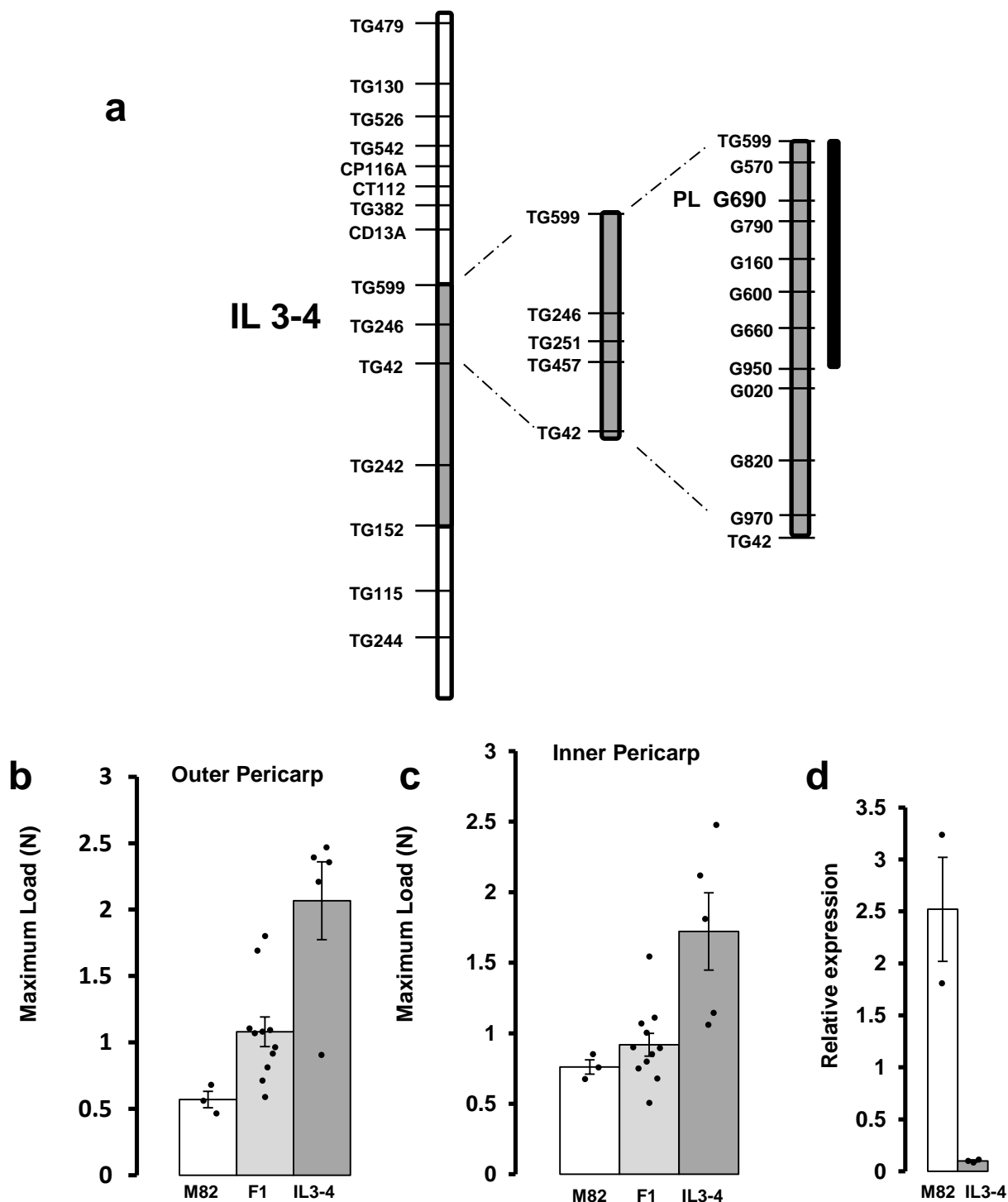


b PL::RNAi parenchyma cell walls



The sections were cut from the pericarp parenchyma cells of **a**, azygous wild type control (WT) or **b**, PL::RNAi line PL5 fruits harvested at red ripe breaker + 7 days. The density of labelling is greater in the PL::RNAi line consistent with reduced degradation of demethylated pectins in these fruits. The micrographs are representative of images taken from pericarp sections of three individual fruit in each treatment.

Supplementary Figure 9: Natural variation for fruit texture associated with PL.



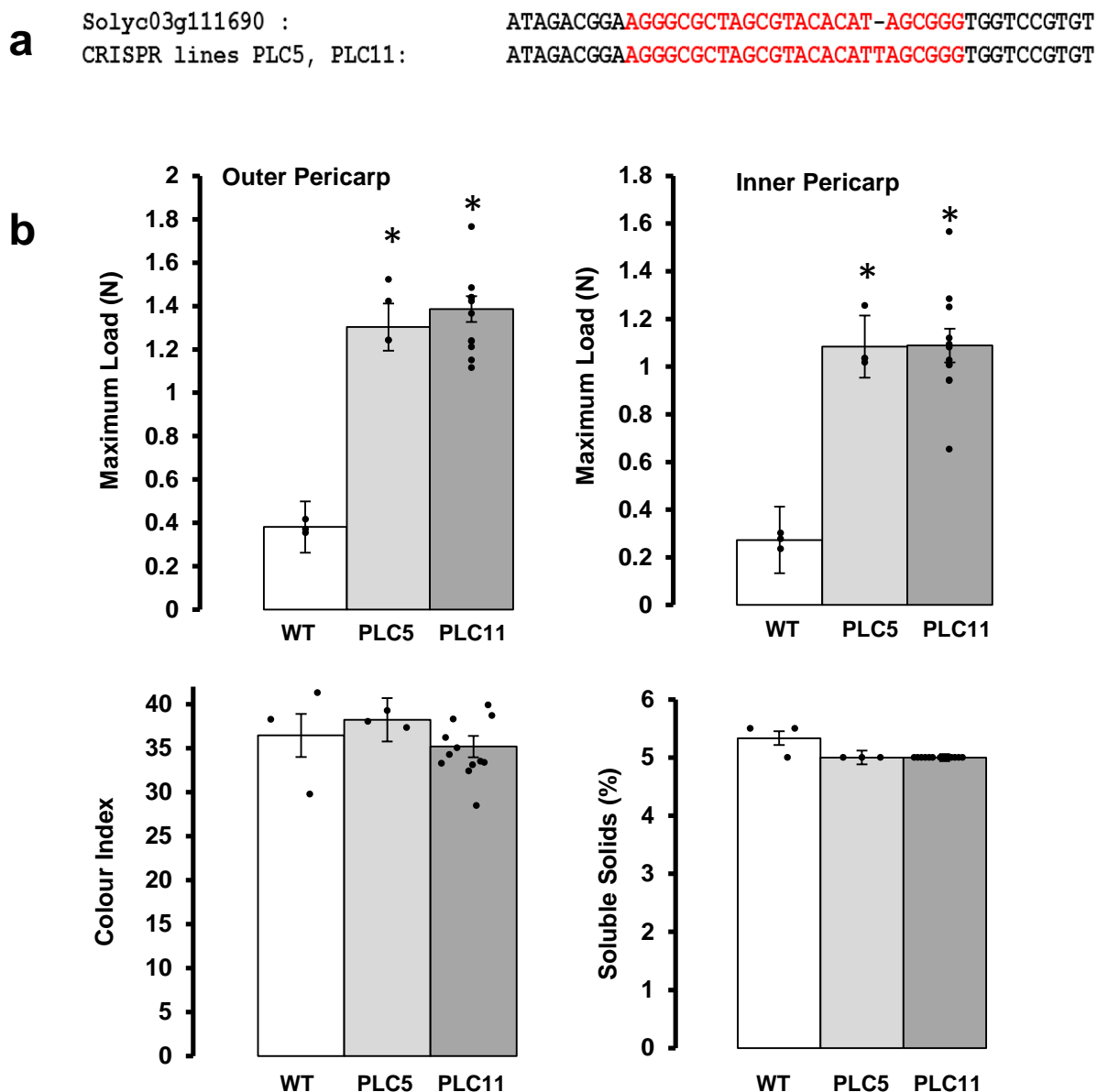
a, Fine mapping of the texture QTL on chromosome 3 and location of the PL locus (marker PLG690). Black bar shows QTL mapping interval of c.1 Mb between TG599 and G950, see Supplementary Figure 10. **b**, texture of the outer and **c**, inner pericarp of fruit of the tomato cultivar M82, IL3-4 (in the M82 background and M82 x IL3-4 F₁ fruits). **d**, PL gene expression at breaker + 7 in M82 and IL3-4. Error bars are s.e.m. For qRT-PCR the means are based on three individual fruit (shown as dots) per genotype. Fruit texture measurements are based on at least 30 individual fruits for each genotype (n=32 for M82, 98 for F₁, and 37 for IL3-4). Dots represent plant means. The texture data were obtained from tomato plants grown in Spring / Summer 2007.

Supplementary Figure 10: Physical structure of key recombinants showing markers used to delineate mapping interval for the fruit firmness QTL on IL3-4.

				Pectate Lyase													
Marker	TG129	TG599	G570	G690*	G790	G160	G600	G640	G660	G750	G950	G020	G820	G970	Number of Fruit	Outer pericarp	Inner pericarp
	61303266	62165453	62187017	62343299	62421266	62659485	62993618	63019083	63030429	63088867	63256776	63322631	65416130	66948553		texture (N)	texture (N)
Plant ID																	
1200															10	0.58	0.97
1831															11	0.48	0.58
1392															11	0.46	0.86
3155															10	0.97	1.17
2877															6	1.16	1.69
1910															10	0.92	1.44
M82															27	0.55	0.84
IL3-4															25	1.42	1.57

The fruit firmness QTL shown in **Supplementary 9** is in a region of the tomato genome with suppressed recombination. The recombinants were identified and the mapping interval determined using markers derived from the tomato genome sequence (G- markers) or from the tomato genetic map (<https://solgenomics.net/> and also see **Supplementary Table 8**). The numbers under each marker are the physical distance in bp along tomato chromosome 3 based on the tomato genome SLv2.50 build (<https://solgenomics.net/>). G690* is a marker in pectate lyase gene. TG599 defines the proximal end of the IL3-4 introgression (<https://solgenomics.net/>). The physical distance between TG599 and G950 = 1091323bp and between TG129 and G950 = 1785601bp. Lines possessing the M82 *S. lycopersicum* allele (red) at G690 were significantly ($P < 0.002$) softer, in both the outer and inner pericarp tissues, than those with the IL3-4 *S. pennellii* allele (green) at the same position. The mean texture values for the outer and inner pericarp (two technical replicates for each measurement) for lines carrying the *S. lycopersicum* and *S. pennellii* alleles at G690 were compared by Analysis of Variance by fitting a linear mixed model with allelic variant as the fixed effect and plant, fruit within plant and technical replicate within fruit as random effects. This ensured that, within the analysis, the variation between means of plants having the different alleles at G690 was compared to the variation between plants of the same genotype at this position. Mean values for the outer pericarp were 0.528 and 1.204N for the lines with *S. lycopersicum* and *S. pennellii* alleles at G690, respectively (SED, 0.1267 with 6 df) and for the inner pericarp the values were 0.817 and 1.480N (SED 0.11862 with 6 df).

Supplementary Figure 11. CRISPR/Cas9-induced mutations in PL in transgenic tomato lines and analysis of pericarp texture and ripening properties



a, Target site for guide RNA (Cas9/sgRNA) used to edit the PL coding sequence by the protocol described in Nekrasov et al ⁴⁵, thirteen transgenic plants harbouring the Cas9 gene were analysed by PCR and sequencing to identify mutations and the lines were then self-pollinated and homozygous mutants were identified by sequencing. Two CRISPR lines, PLC5 and PLC11, from independent transgenic events, yielded the same point mutation and the sequence is shown in comparison to wild type. The single bp insertion results in a stop codon in the PL coding sequence. **b**, Analysis of fruit from lines PLC5 and PLC11 harbouring the PL mutation and the azygous wild type control (WT) revealed fruits with significantly (Ftest; $P \leq 0.04$) firmer texture compared to the control as denoted by *. However there were no significant (Ftest; $P > 0.05$) differences in fruit colour or soluble solids content between PL and WT fruits. Error bars are s.e.m. Dots represent individual fruits. Fruit numbers were WT n=3, PLC11 n=3, PLC 5 n=13.

Supplementary Table 8. Primers for PCR amplification

Primer Name	Forward Primer	Reverse Primer
G570	GGGAGATGGATTTGCTTTCA	GGCCAGACTTTTGACCA
G690 (PL)	ACGCGTTTAATTGGACGTATG	AACAGAGGAAGTGCCC
G790	AAGCCAGAAAGCTTGCGTTA	GCTCAGCTTCAGTGTCAT
G070	GTGTCCGAGGTTTGTCTGTTT	TTAGCGGGCATGTCATT
G160	GCATGCACAATCAGTGAAGG	TCAAAGGGCTGAGGGT
G600	ATTTGTTGATCGCTGGCTTC	CGACGATGGTCAGACC
G640	CAAACTTTGCATTCCATGA	TCTACTGGCAGGAAGG
G660	TGGTTGTTGACCATGAAAA	GGCCATTGAAGCGACA
G750	AGGTTGAATGGGAGTTGCAG	GCAGAAAACCGACTCA
G950	AACTTCAATGGGGCATATCG	TTTGCCACCCCTAATTG
G020	TATATTTGCCCAAGGCACT	ATCGGGACGGATAATG
G820	ATCAATGGCGACTGCTTCTT	TGCCAATTGAACAGGAT
G970	TTCGGTGGATGGTTACAACA	CACCAAAATGCAAGTCA

Primers for RNAi construct and QPCR

2G111690	ACGCGTTTAATTGGACGTATG	AACAGAGGAAGTGCCC
qPL	GCGATCAGGAGTTAGAACTGG	AATCCCCTTTTGCTTTG
qPL probe	TTGAGTTTGAGTGCAAGGCCGTC	
ELF-probe	TCGTTTTGCTGTGAGGGACATGAGGCA	
ELF	ACCTTTGCTGAATACCCTCCATTG	CACAGTTCACTTCCCCT

Name	Accession	Primer efficiency	Forward Pr
PL-like 1	Solyc02g093580	0.94	AAGACGTT
PL-like 2	Solyc03g111690	0.96	CTCGGCCT
PL-like 3	Solyc05g055510	0.95	AGGTGATG
PL-like 4	Solyc06g083580	0.94	CACGCACT
PL-like 5	Solyc09g061890	0.95	AGTCACTT

ATGT
ATTG
TTG
TGA
AGAA
TTTT
AGGA
TATT
GAGG
AAA
TCAC
TGGT
TACG

ATTG
3TT

TCTTCTG

Reverse Primer

GATCCGCACGATAAATAGCC
GCTTGCCTCTCTCTAAAACCAA
GAAATGCAGATTTAGGCTCCA
CCCTGGCTGTTAATTGTAGGA
TGGCTAGACCCAAAAATGGA